

## ORIGINAL ARTICLE

## Blood vessel endothelium-directed tumor cell streaming in breast tumors requires the HGF/C-Met signaling pathway

E Leung<sup>1</sup>, A Xue<sup>1</sup>, Y Wang<sup>1,2</sup>, P Rougerie<sup>1</sup>, VP Sharma<sup>1,3</sup>, R Eddy<sup>1</sup>, D Cox<sup>1,3</sup> and J Condeelis<sup>1,2,3</sup>

During metastasis to distant sites, tumor cells migrate to blood vessels. *In vivo*, breast tumor cells utilize a specialized mode of migration known as streaming, where a linear assembly of tumor cells migrate directionally towards blood vessels on fibronectin-collagen I-containing extracellular matrix (ECM) fibers in response to chemotactic signals. We have successfully reconstructed tumor cell streaming *in vitro* by co-plating tumors cells, macrophages and endothelial cells on 2.5  $\mu\text{m}$  thick ECM-coated micro-patterned substrates. We found that tumor cells and macrophages, when plated together on the micro-patterned substrates, do not demonstrate sustained directional migration in only one direction (sustained directionality) but show random bi-directional walking. Sustained directionality of tumor cells as seen *in vivo* was established *in vitro* when beads coated with human umbilical vein endothelial cells were placed at one end of the micro-patterned 'ECM fibers' within the assay. We demonstrated that these endothelial cells supply the hepatocyte growth factor (HGF) required for the chemotactic gradient responsible for sustained directionality. Using this *in vitro* reconstituted streaming system, we found that directional streaming is dependent on, and most effectively blocked, by inhibiting the HGF/C-Met signaling pathway between endothelial cells and tumor cells. Key observations made with the *in vitro* reconstituted system implicating C-Met signaling were confirmed *in vivo* in mammary tumors using the *in vivo* invasion assay and intravital multiphoton imaging of tumor cell streaming. These results establish HGF/C-Met as a central organizing signal in blood vessel-directed tumor cell migration *in vivo* and highlight a promising role for C-Met inhibitors in blocking tumor cell streaming and metastasis *in vivo*, and for use in human trials.

Oncogene (2017) 36, 2680–2692; doi:10.1038/onc.2016.421; published online 28 November 2016

## INTRODUCTION

During systemic cancer metastasis, tumor cells are relocated from the primary tumor to secondary sites during a process called dissemination,<sup>1–5</sup> resulting in metastasis, which is the major cause of death in breast cancer patients.<sup>6–8</sup> Intravital imaging at single-cell resolution in mammary tumors has shown that dissemination requires cell migration, which involves a change in phenotype from a growing cohesive epithelium to dis cohesive, invasive and migratory tumor cells.<sup>9–13</sup> The end result is the rapid directed migration of tumor cells involved in paracrine signaling chemotaxis, which autonomously form linear patterns called streams.<sup>9,11,14</sup> Streaming cells migrate directionally towards blood vessels at speeds exceeding 3  $\mu\text{m}/\text{min}$  and can intermittently disseminate large numbers of tumor cells to distant sites with rapid kinetics.<sup>15–18</sup>

At the blood vessel surface the streaming tumor cells interact with intravasation doorways called TMEM (tumor microenvironment of metastasis), composed of three cells in direct contact: a Mena-overexpressing tumor cell, proangiogenic TIE2<sup>Hi</sup>/VEGF<sup>Hi</sup> macrophage and the subluminal side of an endothelial cell.<sup>9,18,19</sup> TMEM support transendothelial migration of the tumor cells from the stream. Intravital imaging at single-cell resolution and photo-conversion lineage tracing have shown how single tumor cells within streams interact with TMEM and undergo intravasation at TMEM, thereby causing dissemination into the blood.<sup>18,20</sup> Tumor cells are then carried in the vasculature to distant sites to form metastatic foci.<sup>21,22</sup> In breast tumors, transient vascular

permeability and its associated tumor cell intravasation occur only at TMEM.<sup>18</sup> The number of TMEM structures in the breast tumor is predictive of distant metastasis in breast cancer patients.<sup>23–25</sup>

Investigating the mechanisms and signals that govern how tumor cells move within the primary tumor towards blood vessels is essential in order to understand and prevent metastatic dissemination. Previous work has identified some of the signals involved in streaming migration.<sup>10,15,26,27</sup> Streaming tumor cells migrate along fibronectin-containing collagen1 fibers that serve as highways directed towards the blood vessels.<sup>14,28,29</sup> Macrophages aid in this streaming phenomenon via the epidermal growth factor (EGF)-colony-stimulating factor 1 (CSF1) paracrine loop, where the tumor cells secrete CSF1 but express epidermal growth factor receptor (EGFR) and the macrophages secrete EGF but express colony-stimulating factor 1 receptor (CSF1R) to form pairs of macrophages and tumor cells mutually attracted by this paracrine signaling loop.<sup>26,30</sup> In inflammatory human breast cancer, the tumor cells themselves may also express CSF1R, leading to an autocrine signal between tumor cells, resulting in the pairing of tumor cells to form streams independently of macrophages.<sup>10,31</sup>

A commonly observed type of streaming in both human and rodent mammary tumors involves paired tumor cells and macrophages, where these pairs form linear streams of tumor cells and macrophages that migrate towards blood vessels.<sup>11,15</sup> The formation of pairs and streams from these heterogeneous cell interactions is a highly organized cell autonomous phenomenon

<sup>1</sup>Department of Anatomy and Structural Biology, Albert Einstein College of Medicine, Bronx, NY, USA; <sup>2</sup>Integrated Imaging Program, Albert Einstein College of Medicine, Bronx, NY, USA and <sup>3</sup>Gruss Lipper Biophotonics Center, Albert Einstein College of Medicine, Bronx, NY, USA. Correspondence: Professor J Condeelis, Department of Anatomy and Structural Biology, Albert Einstein College of Medicine, 1301 Morris Park Avenue, Price 208, Bronx, NY 10461, USA.  
E-mail: john.condeelis@einstein.yu.edu

Received 12 April 2016; revised 13 September 2016; accepted 30 September 2016; published online 28 November 2016

involving signaling rules that have been elucidated both experimentally and with mathematical models.<sup>14,32</sup> As a result, pairing and streaming can be reconstituted from purified tumor cells and macrophages when placed on either fibronectin-collagen1 fibers or fibronectin-collagen1 strips *in vitro*.<sup>14,33</sup>

Expression profiling of the tumor cells involved in streaming migration and TMEM function reveals an increase in expression of genes associated with the Mena–Cofilin pathway that regulates actin polymerization during chemotaxis and invasion of tumor cells.<sup>11,34,35</sup> Mena is an actin-binding protein that is involved in the regulation of Cofilin-stimulated actin polymerization.<sup>36,37</sup> This pathway causes the localized activation of Cofilin's actin polymerization activity, thereby regulating chemotaxis and invadopodium assembly.<sup>38,39</sup> Of particular significance to the mechanism of streaming and tumor cell dissemination is the finding that Mena is differentially spliced in streaming and disseminating tumor cells showing the splicing pattern Mena<sup>INV-high</sup>/Mena11a<sup>low</sup>.<sup>9,20,40</sup>

The Mena<sup>INV</sup> isoform has been shown to increase the amount of tumor cell streaming, invasion and dissemination *in vivo* when overexpressed in tumor cells.<sup>9,19,41</sup> One mechanism by which Mena enhances tumor cell invasion and migration is through the sensitization of tumor cells to ligands for receptor tyrosine kinases such as EGF and hepatocyte growth factor (HGF).<sup>41,42</sup> The enhanced sensitivity to EGF increases the ability of tumor cells to degrade matrix, thereby facilitating invasion, and to also interact with macrophages to form migrating streams.<sup>19,42</sup> The splicing pattern Mena<sup>INV-high</sup>/Mena11a<sup>low</sup> is correlated with TMEM assembly and is required for macrophage-induced transendothelial migration in TMEM.<sup>20</sup> These results explain why the Mena<sup>INV-high</sup>/Mena11a<sup>low</sup> splicing pattern is predictive of metastatic relapse and poor survival in breast cancer patients.<sup>43,44</sup>

Previous work has shown that, while the EGF-CSF1 paracrine loop between the tumor cells and macrophages mediates pairing and stream formation,<sup>10,11,14,19</sup> these signals alone are not sufficient for sustained directional migration (sustained directionality) towards blood vessels. Further study has distinguished additional signals that are involved in streaming from those that are not. For example, TIE2, VEGF and CXCL12 (SDF1) signaling are all involved in tumor cell-blood vessel interactions and invasion<sup>18,35,41,45,46</sup> and HGF lies at the center of signaling interactions predicted in streaming tumor cells.<sup>35</sup> Patients with increased C-Met expression have overall worse survival.<sup>45</sup> Furthermore, it has been demonstrated that Mena<sup>INV</sup> overexpression is present in streaming tumor cells<sup>19,40</sup> and that Mena<sup>INV</sup> enhances the sensitivity of tumor cells towards both EGF and HGF, identifying both signals as possible candidates for regulating directional migration of tumor cell streams towards blood vessels.<sup>41</sup> In this paper, we have investigated the importance of HGF signaling in the directional migration of breast tumor cells and how it might be integrated with the CSF1/EGF paracrine signaling loop to organize streaming towards blood vessels *in vivo*.

## RESULTS

Sustained directionality of tumor cell migration requires additional signals beyond the CSF1/EGF paracrine loop

Previously, we established an *in vitro* linear micro-patterned substrate assay (1D assay) to reconstitute macrophage and tumor cell interactions observed on fibronectin-collagen1 fibers in mammary tumors *in vivo*.<sup>14,33</sup> Using this assay, we were able to recapitulate the *in vivo* findings that tumor cells and macrophages interact and migrate towards each other to form pairs using the EGF/CSF1 paracrine loop and that the pairs form linear streams of cells, aligned on fibronectin collagen-containing fibers, with elevated velocity and persistence over short intervals of

time.<sup>14,33</sup> Here we have repeated this assay and, while the previous results were confirmed, we found that the pairing and streaming formed in response to EGF/CSF1 paracrine signaling alone was not sufficient to support sustained directionality of either cell type (Figure 1 and Supplementary Movie 1). This is in stark contrast to what is observed *in vivo*, where tumor cells and their associated macrophages directionally migrate towards blood vessels over long periods of time.<sup>19,47,48</sup>

Sustained directionality of tumor cell migration requires endothelial cells and is distance dependent

Since tumor cells preferentially migrate towards blood vessels *in vivo*, we hypothesized that endothelial cells contribute to sustained tumor cell directionality. To test this hypothesis, human umbilical vein (HUVEC) endothelial cells coated onto Sephadex beads were added into the 1D assay with the tumor cells. We observed that tumor cells exhibit sustained directionality of streaming towards the endothelial cells (Figures 2a and d and Supplementary Movie 2), but if the tumor cells were more than 500  $\mu\text{m}$  away from the bead, sustained directionality was no longer observed (Figures 2b and d and Supplementary Movie 3). However, adding macrophages allowed the tumor cells to exhibit sustained directionality towards the endothelial cells beyond the 500  $\mu\text{m}$  distance from the endothelial cells (Figures 2c and d and Supplementary Movie 4).

Endothelial cells signal directional migration using soluble HGF

To identify the signal from endothelial cells causing directional migration of tumor cell streams, Boyden chambers were set up as shown in Figure 3a, where tumor cells were plated on top of the membrane and HUVEC cells or HUVEC conditioned media (CM) were plated at the bottom of the well. The tumor cells were able to migrate towards the endothelial cells and towards the HUVEC conditioned media (Figure 3b), suggesting that the signal is a soluble factor secreted into the media by the endothelial cells. This effect was not tumor cell line specific since both human MDA-MB-231 and rat MTLn3 breast tumor cells were also able to migrate towards HUVEC cells (Supplementary Figures S1A and B and Supplementary Movie 1). In addition, MTLn3 cells were able to migrate towards both HUVEC and rat lung micro-vascular endothelial primary cells (Supplementary Figures S1C).

Based on the signaling pathways implicated in the breast tumor Invasion Signature,<sup>15,34,35,49</sup> potential candidate signaling molecules were tested, including SDF-1, HGF, Ang1, Ang2, VEGF, EGF and CSF-1 (Figure 3b). Out of these candidate signaling molecules, addition of HGF or EGF to the bottom well produced the most robust migration of tumor cells. EGF has been previously described as an important chemoattractant for tumor cell migration<sup>9,50</sup> and inhibiting EGF with 1  $\mu\text{M}$  Iressa blocked migration as expected (Figure 3b). The role of HGF in directed tumor cell migration towards endothelial cells, however, is less well documented. As such, we performed western blots for HGF and C-Met (HGF receptor) to confirm that tumor cells have the receptor to HGF (C-Met) and endothelial cells produce HGF. In addition, tumor cells were found to express HGF (Figure 3c). While tumor cells expressed both HGF and C-Met, the migration of the tumor cells in response to autocrine HGF was less compared to tumor cell migration towards endothelial cells (Figure 3d). When C-Met inhibitors PF04217903<sup>51–53</sup> and Altiratinib<sup>54</sup> were added to the transwells, tumor cell migration towards the HUVEC conditioned media was inhibited (Figure 3e).

To assess the relative importance of HGF secreted from either tumor cells or endothelial cells, ELISA assays were performed. HGF secretion by HUVECs was measured to be around 46.5  $\mu\text{M}$  by ELISA (Supplementary Figure S3A). HGF secretion by MTLn3 tumor cells was measured to be around 4.6  $\mu\text{M}$ , which is below the reported Kd value (30  $\mu\text{M}$ ) for the high-affinity C-MET receptor.<sup>55,56</sup> Using

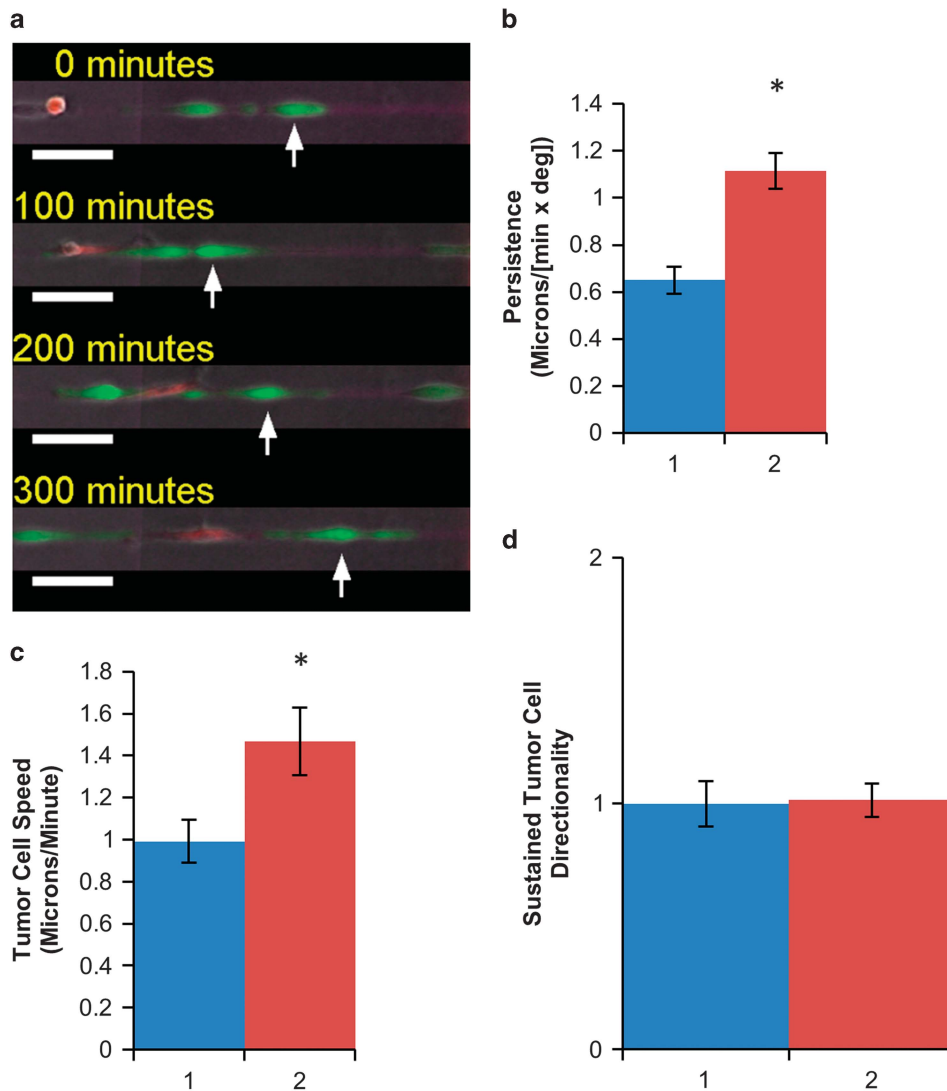


**Figure 1.** Tumor cells pair with macrophages but do not exhibit sustained directionality. **(a)** In the 1D assay, MTLn3 tumor cells (green) interact with bone marrow derived macrophages (BMMs; red) and form pairs of macrophages and tumor cells. White arrow = MTLn3 tumor cell position. Magenta = 1D fibronectin track. White scale bar = 50  $\mu$ m. **(b)** MTLn3 tumor cells in the presence of BMMs show higher persistence ‡ compared to MTLn3 tumor cells alone; (1) MTLn3 tumor cells alone; (2) MTLn3 tumor cells+BMMs. ‡ Persistence is calculated as velocity/  $(1+(100/360) \times \text{angle})$ . Mean  $\pm$  s.e.m., *t*-test  $*P < 0.05$ ; *n* = 100 cells per condition; four independent experiments. **(c)** Similarly, MTLn3 tumor cells in the presence of BMMs, have increased tumor cell speed compared to MTLn3 tumor cells alone; (1) MTLn3 tumor cells alone; (2) MTLn3 tumor cells+BMMs. Mean  $\pm$  s.e.m., *t*-test  $*P < 0.05$ ; *n* = 100 cells per condition; four independent experiments. **(d)** However, MTLn3 tumor cells display no change in sustained directionality †† even in the presence of macrophages and remain at the baseline motility value defined below; (1) MTLn3 tumor cells alone; (2) MTLn3 tumor cells+BMMs. †† Sustained directionality is calculated as the net path length over the total path length during the course of the 8h movie. Values are normalized to tumor cell baseline motility. A value of 1 represents baseline motility with no sustained directionality. Mean  $\pm$  s.e.m., *t*-test  $*P < 0.05$ ; *n* = 100 cells per condition; four independent experiments.

these ELISA values, the local concentration of HGF secreted from the endothelial cell beads and from MTLn3 tumor cells in the 1D assay was calculated (Supplementary Materials and Methods). These calculations reveal that the HUVEC endothelial cell beads can secrete around 2.1 nM HGF into the media while tumor cells in the same volume secrete ~1.4  $\mu$ M of HGF into the 1D assay. The numbers suggest that MTLn3 tumor cells would not be able to sense the autocrine tumor cell source of HGF compared to the paracrine HGF.

Recent evidence has demonstrated that TIE2 and VEGFR2 are associated with tumor cell dissemination at the blood vessel endothelium.<sup>18</sup> We found that inhibiting TIE2 and VEGFR2 receptors with Rebastinib and VEGFR2 blocking antibodies at the concentrations near the IC50<sup>57–60</sup> and ND50<sup>61–64</sup> and sufficient

to inhibit vascular permeability and intravasation *in vivo*<sup>18</sup> had no effect on tumor cell migration (Figure 3e).

However, knockdown of C-Met in the tumor cells blocked the migration of tumor cells towards HUVEC endothelial cells in transwells (Figures 3f and g). Knockdown of HGF in the HUVEC cells inhibited the migration of tumor cells towards endothelial cells in transwells (Supplementary Figure S3B). When macrophages were added to the bottom chamber with endothelial cells, more pronounced migration of tumor cells occurred (Supplementary Figure S3b, bar 6). When macrophages were added to the bottom chamber with endothelial cells that had HGF knocked down, tumor cells migrated towards the bottom of the transwell at the level seen in wells containing only macrophages (Supplementary Figure S3B, bars 7 and 8).

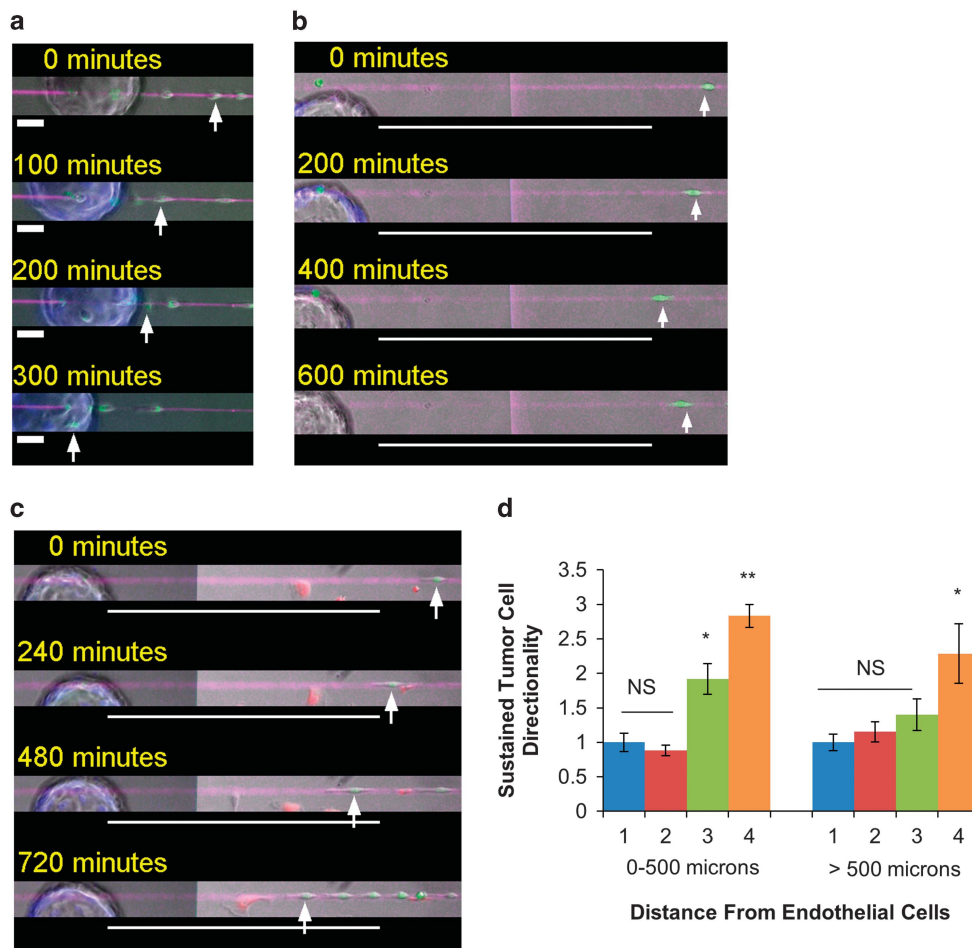


**Figure 2.** Tumor cells exhibit sustained directional streaming towards endothelial cells in a distance dependent relationship. (a) MTLn3 tumor cells (white arrow) migrate on the micro-patterned substrates (magenta line) towards HUVEC endothelial cells on a bead. White scale bar = 50  $\mu$ m. (b) When the MTLn3 tumor cells are more than 500  $\mu$ m away from the HUVEC bead, the MTLn3 tumor cells lose their sustained directionality towards the HUVEC endothelial cells on a bead (white arrow = MTLn3 tumor cell position, magenta line = fibronectin track, bead = HUVEC endothelial cells, white scale bar = 500  $\mu$ m). (c) When macrophages (red) are added, the tumor cells (white arrow) that are more than 500  $\mu$ m away migrate towards the HUVEC endothelial cells. White scale bar = 500  $\mu$ m. (d) Quantification of sustained tumor cell directionality reveals that macrophages enhance sustained tumor cell directionality  $\ddagger$  towards the HUVEC endothelial cell beads. (1) MTLn3 tumor cells alone; (2) MTLn3 tumor cells+BMMs; (3) MTLn3 tumor cells+HUVECs; (4) MTLn3 tumor cells+BMMs+HUVECs.  $\ddagger$  Sustained directionality is calculated as the net path length over the total path length during the course of the 8 h movie. Values are normalized to tumor cell baseline motility. A value of 1 represents baseline motility with no net sustained directional migration. Mean  $\pm$  s.e.m., ANOVA \* $P$  < 0.001 \*\* $P$  value < 0.0005 relative to bar 1.  $n$  = 16 cells analyzed per condition; 4–5 independent experiments.

Chemotactic index, a measure of the ability of crawling cell to follow a chemotactic gradient, was determined for tumor cells in response to HGF stimulation. The chemotactic index was calculated as described in Supplementary Figure S2C and previously.<sup>65–67</sup> Tumor cells demonstrated significant chemotaxis to gradients of HGF delivered from a point source (Supplementary Movie 2), and had a higher chemotactic index compared to control cells and SDF1 stimulated tumor cells (Supplementary Movie 3 and Supplementary Figures S2D and E), demonstrating that the directional migration to HGF is a chemotactic response. The ability of tumor cells to have a high chemotactic index in response to HGF demonstrates that tumor cells are not simply undergoing chemokinetic responses to HGF. This is consistent with the finding that when HGF is placed in both the top and bottom chambers of the transwell, the ability of tumor cells to undergo efficient chemotaxis towards the bottom of the transwell was abolished (Supplementary Figure S2A). These results strongly implicate the HGF/C-Met signaling axis in tumor cell chemotaxis towards endothelial cells.

Sustained directionality towards endothelial cells is inhibited by blocking HGF/C-Met signaling

To confirm that the C-Met/HGF signaling axis is required for sustained tumor cell directionality towards endothelial cells, sustained directionality of tumor cells towards endothelial cells was measured in the 1D assay (Figure 4). We found that sustained tumor cell directionality could be inhibited by knocking down the C-Met receptor in the tumor cells (Figures 4a and b) or knocking down HGF in the HUVEC endothelial cells (Figures 4c–f, Supplementary Figures S3C and D) but not by knocking down the HGF in the tumor cells (Supplementary Figure S5). These results are consistent with the Boyden chamber results above and the calculations of the relative amounts of HGF secretion by endothelial cells and tumor cells (Supplementary Materials and Methods) which concluded that tumor cell secreted HGF is not a detectable signal during sustained directional migration of tumor cells towards endothelial cells.

We next tested the C-Met inhibitors PF04217903<sup>51–53</sup> and Altiratinib<sup>54</sup> in the 1D assay to assess their effects on sustained



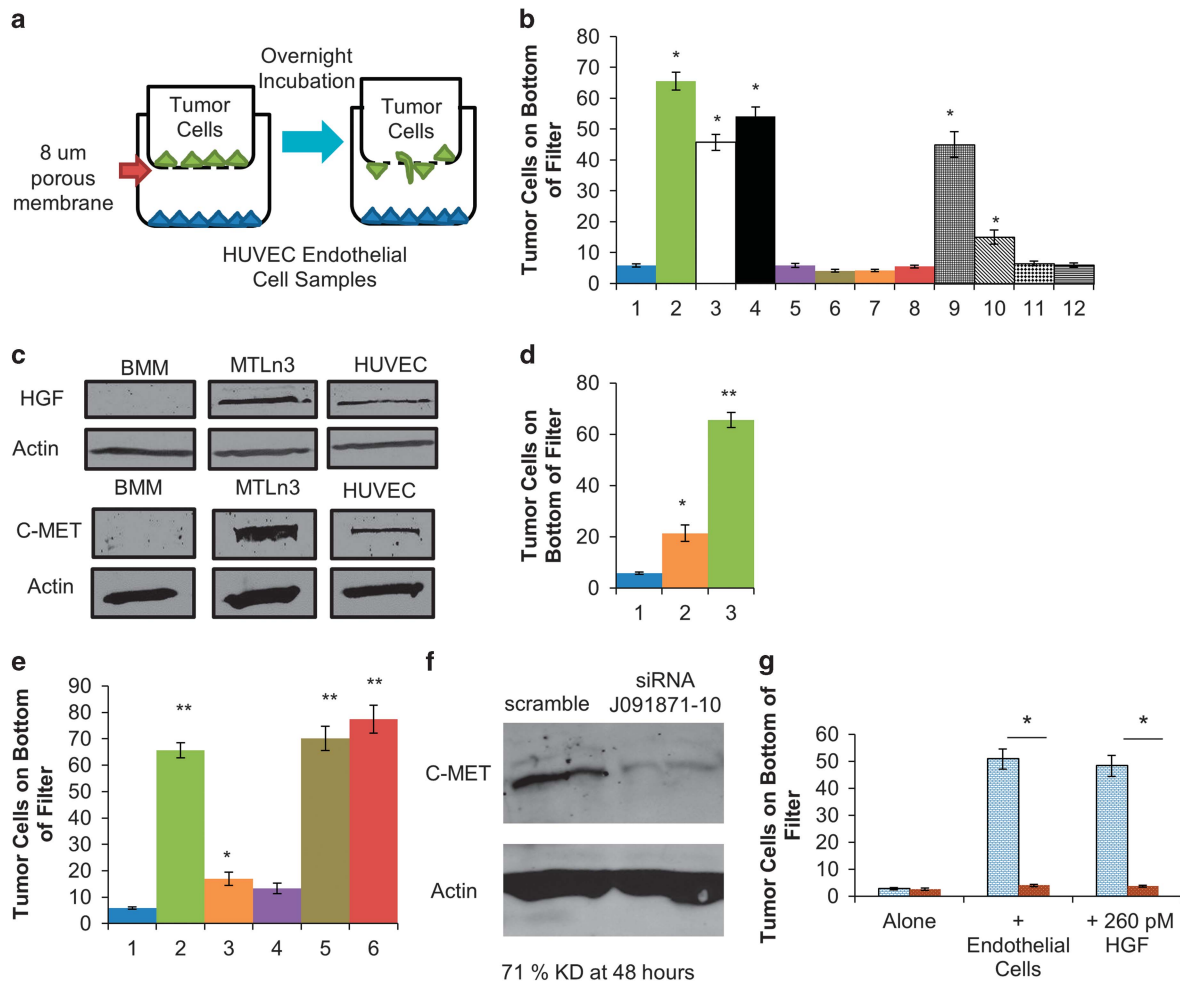
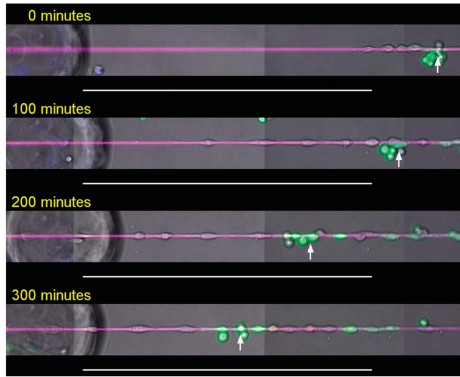


**Figure 3.** Tumor cells migrate towards endothelial cells in response to the HGF/C-Met signaling pathway. **(a)** To determine the signal responsible for tumor cell migration towards the HUVEC endothelial cells, Boyden chambers were utilized where HUVEC endothelial cells were plated on the bottom of the well and MTLn3 tumor cells were plated on top. **(b)** Quantification of the Boyden Chambers reveals that MTLn3 tumor cells migrate towards HUVEC Endothelial cells. (1) MTLn3 tumor cells in the top well in EGM2 media; (2) MTLn3 tumor cells in the top well with HUVEC endothelial cells in the bottom of the well; (3) MTLn3 tumor cells in the top well with HUVEC Conditioned Media in the bottom of the well (4) MTLn3 tumor cells in the top well with 260 pM HGF in the bottom of the well (5) MTLn3 tumor cells in the top well with 1 nM SDF-1 in the bottom of the well (6) MTLn3 tumor cells in the top well with 5 nM Ang1 in the bottom of the well (7) MTLn3 tumor cells in the top well with 5 nM Ang2 in the bottom of the well (8) MTLn3 tumor cells in the top well with 500 nM VEGF in the bottom of the well (9) MTLn3 tumor cells in the top well with 5 nM EGF in the bottom of the well (10) MTLn3 tumor cells in the top well with 5 nM EGF and 1 μM Iressa in the bottom of the well (11) MTLn3 tumor cells in the top well with 1 nM CSF1 in the bottom of the well (12) MTLn3 tumor cells in the top well with 1 nM CSF1 and 10 nM DCC-3014 (CSF1R inhibitor) in the bottom of the well. The concentrations of VEGF, Ang1, Ang2, SDF-1, EGF, and CSF-1 used in the assay are near the reported KD values of the receptors.<sup>83–88</sup> Mean ± s.e.m., ANOVA. \**P* < 0.05 relative to bar 1. *n* = 150 fields of view per condition; 3–6 independent experiments. **(c)** Western blot analysis of HUVEC endothelial cells and MTLn3 tumor cell lysates show that MTLn3 tumor cells and HUVEC cells express the C-Met receptor and HGF. **(d)** While MTLn3 tumor cells express HGF and C-Met receptor, the migration of MTLn3 tumor cells in an autocrine fashion is not as effective as MTLn3 tumor cell migration towards HUVEC endothelial cells in the transwell assay described in **(a)**. (1) MTLn3 alone in top well (2) MTLn3+MTLn3 in top and bottom wells, respectively (3) MTLn3+HUVEC in top and bottom wells, respectively. Mean ± s.e.m. ANOVA \**P* < 10<sup>−4</sup> \*\**P* < 10<sup>−10</sup> relative to bar 1. *n* = 150 fields of view per condition. 5–6 independent experiments. **(e)** The migration of MTLn3 tumor cells towards HUVECs is inhibited by the C-Met inhibitors PF04217903 and Altiratinib. (1) MTLn3 in the top well with EGM2 media; (2) MTLn3+HUVECs, top and bottom wells, respectively; (3) MTLn3+HUVEC, top and bottom wells, respectively, +5 nM C-Met inhibitor Altiratinib; (4) MTLn3+HUVEC, top and bottom wells, respectively, +7 nM C-Met inhibitor PF04217903; (5) MTLn3+HUVEC, top and bottom wells, respectively, +5 nM Rebastinib (TIE2i); (6) MTLn3+HUVEC, top and bottom wells, respectively; +0.25 μg/ml VEGFR2 neutralizing antibody. Mean ± s.e.m., ANOVA. \**P* < 0.05; \*\**P* < 10<sup>−3</sup> relative to bar 1. *n* = 90 fields of view per condition; 3–6 independent experiments. **(f)** Knockdown of expression of the C-Met receptor in MTLn3 tumor cells using siRNA J091871-10 led to a 71% reduction in C-Met receptor expression. **(g)** Using these C-Met knockdown tumor cells in the Boyden chamber assay reduces the ability of the MTLn3 tumor cells to migrate towards HUVEC endothelial cells at the bottom as well as towards HGF. Blue hash tag bar = parental MTLn3 transfected with Scrambled siRNA. Orange dotted bar = C-Met KD in MTLn3 cells transfected with siRNA J091871-10 targeting C-MET receptor. Mean ± s.e.m., ANOVA \**P* < 10<sup>−6</sup>; *n* = 90 fields of view per condition; three independent experiments.

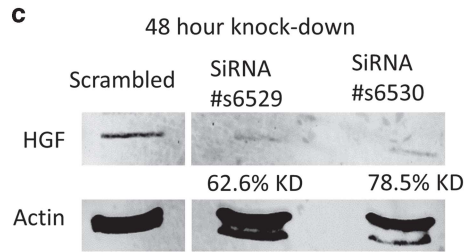
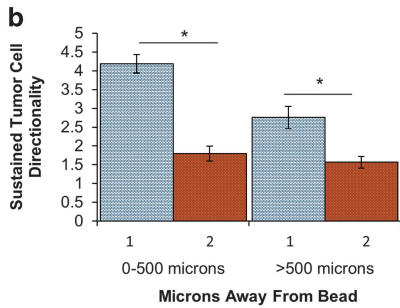
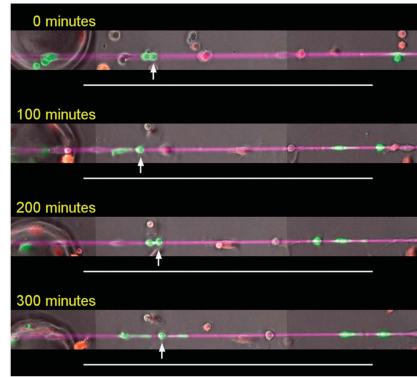
directional migration towards endothelial cells. The inhibition of C-Met with these inhibitors abolished the sustained tumor cell directionality (Figures 4g and i). Inhibition of EGFR and CSF1R also reduced the sustained directionality of tumor cells but, unlike inhibition of C-Met, did not completely abolish sustained

directionality of tumor cells (Figures 4h and i). While this result is in agreement with prior work implicating a paracrine chemotaxis signaling loop in tumor cell streaming *in vivo*,<sup>9,10</sup> it also indicates that HGF is the main signal involved in sustained directionality towards endothelial cells.

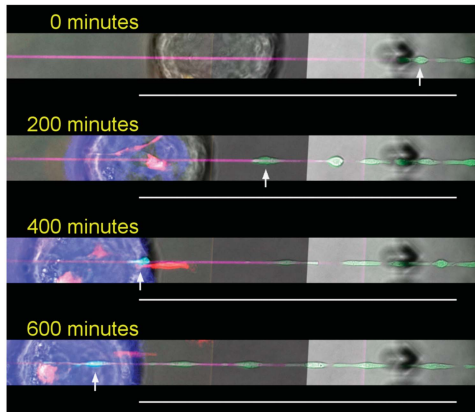
**a** BMMs + HUVEC Bead + MTLn3 Tumor cells transfected with scrambled siRNA



BMMs + HUVEC Bead + MTLn3 Tumor cells transfected with siRNA J091871-10 targeting C-MET



**d** MTLn3 Tumor cells + BMM + HUVECs transfected with scrambled siRNA



**e** MTLn3 Tumor cells + BMM + HUVECs transfected with siRNA #s6529 targeting HGF

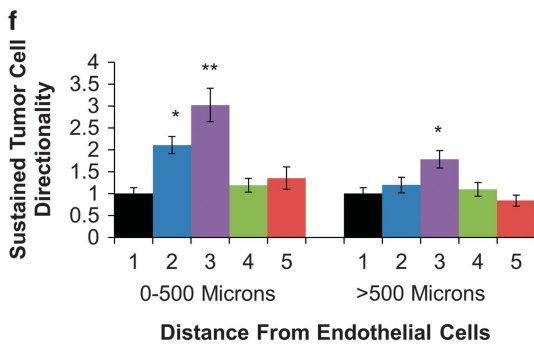
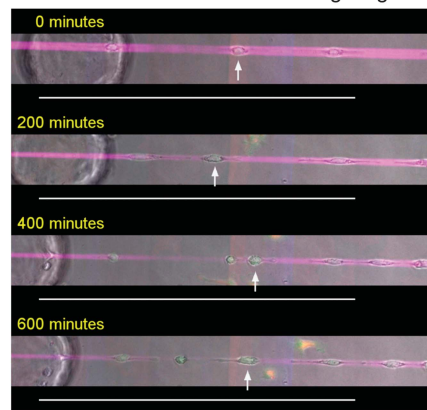
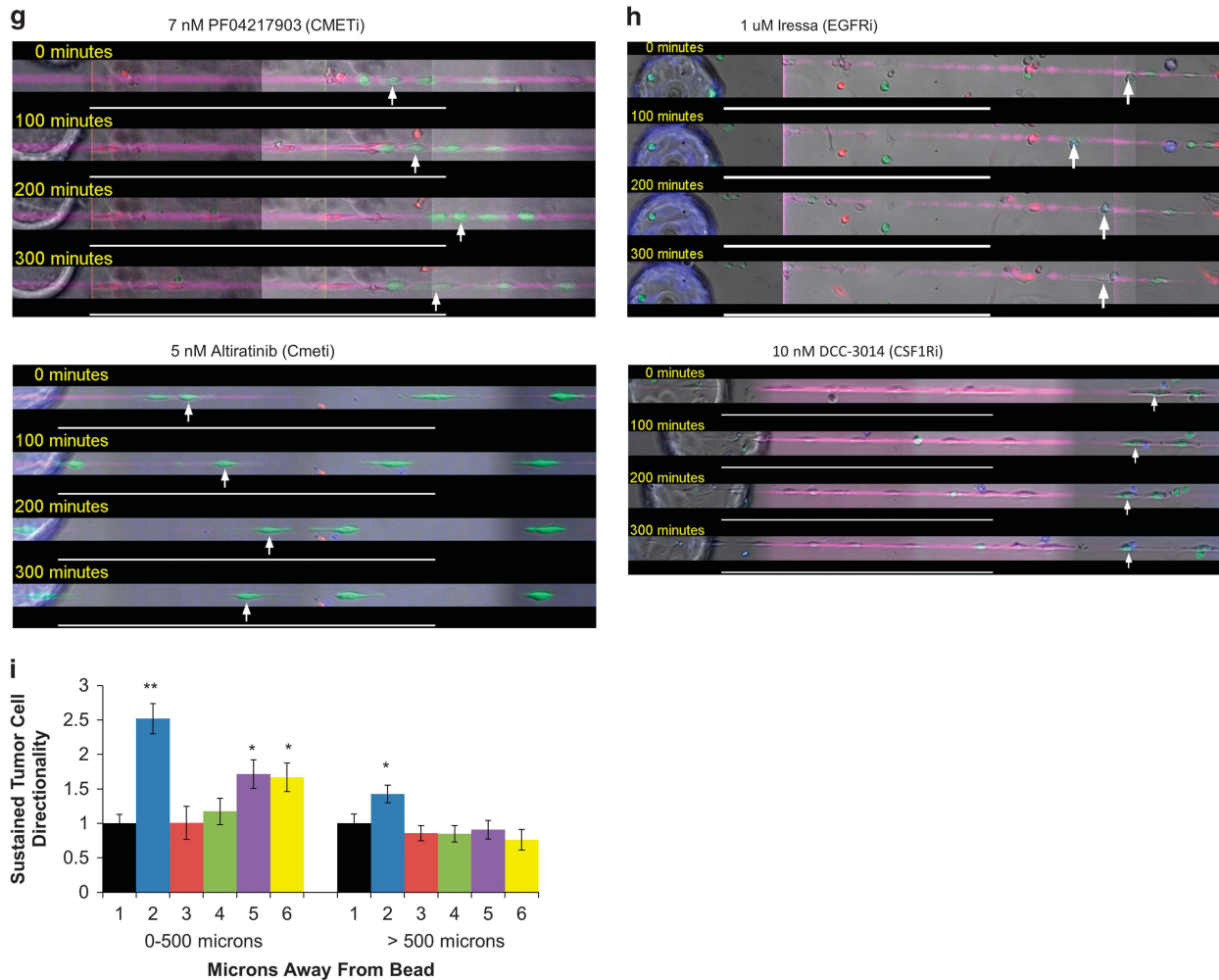


Figure 4. Continued.



**Figure 4.** Sustained directionality towards endothelial cells is inhibited by blocking HGF/C-Met signaling and reduced by inhibition of the EGF/CSF-1 paracrine loop. **(a)** Knockdown of C-Met receptor in MTLn3 tumor cells reduces the ability of MTLn3 tumor cells to exhibit sustained directionality towards HUVEC endothelial cells even in the presence of macrophages in the 1D streaming assay. Left panel—BMMs+HUVEC endothelial cell bead+MTLn3 tumor cells transfected with scrambled siRNA. Right panel—BMMs+HUVEC endothelial cell bead+MTLn3 tumor cells transfected with siRNA J091871-10 targeting C-MET receptor (Figure 3f). Green = MTLn3 tumor cells. Red = BMMs. Blue = HUVEC endothelial cell bead. Magenta = fibronectin track. White arrow = MTLn3 tumor cell position. **(b)** Quantification of sustained tumor cell directionality from **(a)**. (1) Parental MTLn3 transfected with scrambled siRNA+BMMs+HUVEC beads; (2) C-Met siRNA KD MTLn3 cells+BMMs+HUVEC beads. Sustained directionality values are normalized to baseline tumor cell motility. Mean  $\pm$  s.e.m., ANOVA  $*P < 0.005$ ;  $n = 50$  cells analyzed per condition; three independent experiments. **(c)** Western blot of HGF in HUVEC endothelial cells transfected with siRNA against HGF. siRNA #s6529 achieved 62% knockdown efficiency while siRNA #s6530 achieved 78% efficacy in knockdown. Use of siRNA #s6529 is shown in **(e, f)** and use of siRNA #s6530 is shown in Supplementary Figures S3C and D. **(d)** MTLn3 tumor cells (green) migrate with sustained directionality towards HUVECs transfected with scrambled siRNA (blue bead) in the presence of macrophages (red) on the 1D fibronectin track (magenta). White arrow = MTLn3 tumor cell position. **(e)** HUVECs transfected with siRNA #s6529 targeting HGF do not support sustained tumor cell directionality. Green = MTLn3 tumor cells. Blue bead = HUVEC bead. Red = BMMs. Magenta = 1D fibronectin track. White arrow = MTLn3 tumor cell position. **(f)** Quantification of tumor cell sustained directionality from **(d)** and **(e)** demonstrates inhibition of sustained tumor cell directionality when HGF is knocked down in HUVEC endothelial cells. (1) MTLn3 tumor cells alone; (2) MTLn3 tumor cells +HUVEC endothelial cells transfected with scrambled siRNA; (3) MTLn3 tumor cells+BMMs+HUVEC endothelial cells transfected with scrambled siRNA; (4) MTLn3 tumor cells+HUVEC endothelial cells transfected with siRNA #s6529; (5) MTLn3 tumor cells+BMMs+HUVEC endothelial cells transfected with siRNA #s6529. Sustained directionality values are normalized to baseline tumor cell motility. See Supplementary Figure S3C and D for similar results with siRNA #s6530. Mean  $\pm$  s.e.m., ANOVA  $*P < 0.05$ ;  $**P < 10^{-5}$  relative to bar 1.  $n = 17$  cells analyzed per condition; four independent experiments. **(g)** In the *in vitro* 1D streaming assay, addition of PF04217903 or Altiratinib (C-METi) blocks sustained directionality of MTLn3 tumor cells (white arrow) towards endothelial cells at all distances. **(h)** Iressa and DCC-3014 block sustained directionality of tumor cells (white arrow) at distances greater than 500  $\mu$ m away from HUVEC endothelial cells. **(i)** Inhibiting C-MET signaling abolishes sustained tumor cell directionality towards HUVEC endothelial cells while inhibition of EGF and CSF1 signaling reduces or blocks sustained tumor cell directionality within, and beyond 500  $\mu$ m, respectively. (1) MTLn3 tumor cells alone (baseline motility); (2) MTLn3+HUVEC endothelial cell bead+BMMs+DMSO vehicle; (3) MTLn3+HUVEC endothelial cell bead+BMMs+7 nM C-Met inhibitor PF04217903; (4) MTLn3+HUVEC endothelial cell bead+BMMs+5 nM C-Met inhibitor Altiratinib; (5) MTLn3+HUVEC endothelial cell bead+BMMs+1  $\mu$ M EGFR inhibitor Iressa; (6) MTLn3+HUVEC endothelial cell bead+BMMs+10 nM CSF1R inhibitor DCC-3014. All values are normalized to the baseline tumor cell motility in bar #1. All drugs were used at concentrations that were previously published to be maximally effective at inhibiting their respective receptors. Mean  $\pm$  s.e.m., ANOVA.  $**P < 0.001$ ;  $*P < 0.05$  relative to baseline tumor cell motility in bar 1.  $n = 13$  cells analyzed per condition; 3–5 independent experiments.

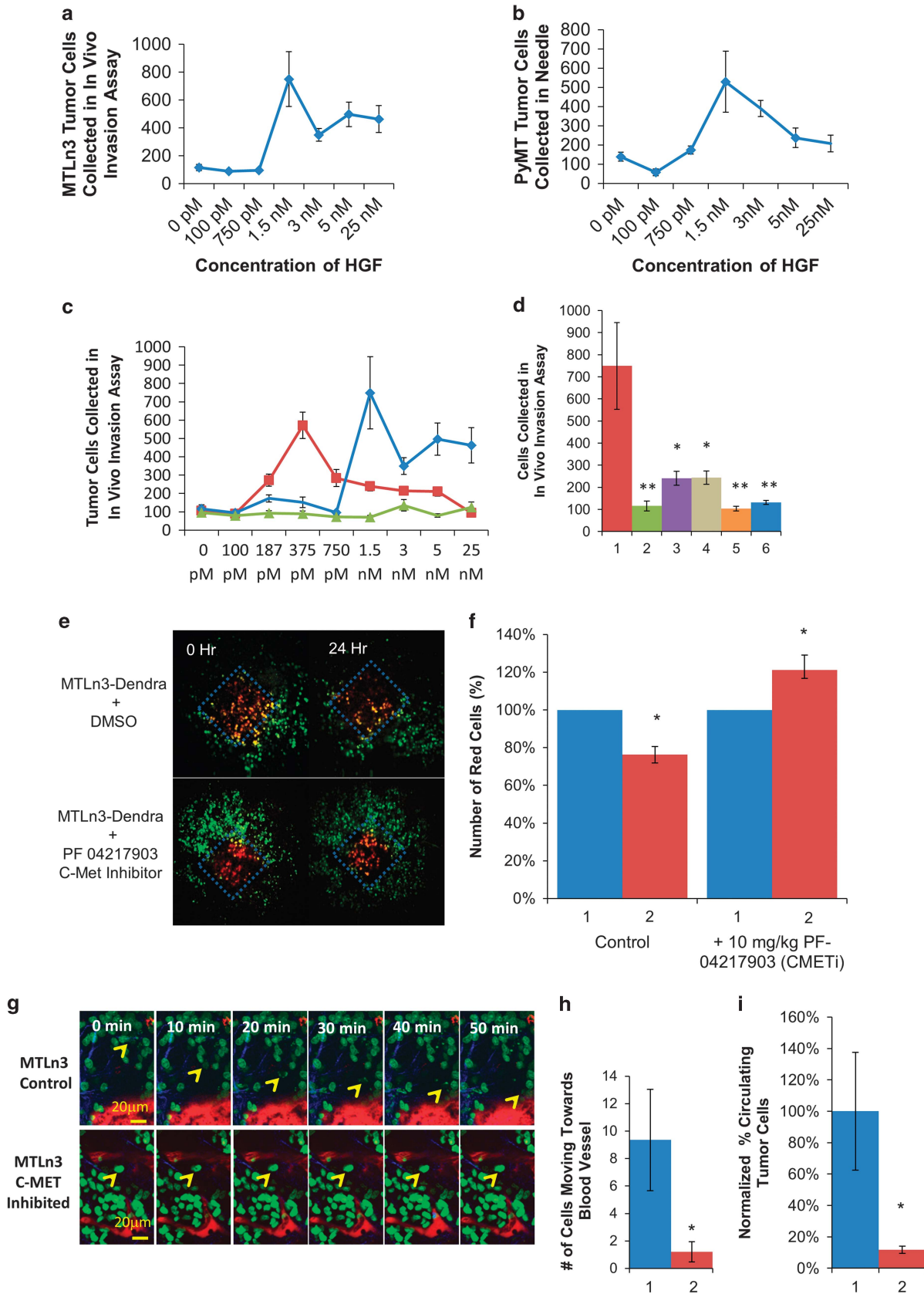


Figure 5. For caption see page 2688.



### C-Met inhibition affects tumor cell migration *in vivo*

The results above point to a central role for HGF in sustained tumor cell directionality during streaming migration of tumor cells towards endothelial cells. The key question is 'Does HGF play the same role in sustained directional migration of tumor cells *in vivo*?' We investigated this using the *in vivo* invasion assay<sup>19,68</sup> and via intravital imaging. Using the *in vivo* invasion assay, we found that in both orthotropic MTLn3 tumors and spontaneous PyMT tumors tumor cells migrate towards HGF *in vivo*, demonstrating the usual biphasic dose response curve that peaks near the center of the chemotactic dose response as described previously<sup>19</sup> (Figures 5a and b). MTLn3 tumor cells could be further sensitized towards HGF *in vivo* when they were overexpressing Mena<sup>INV</sup> but not Mena11a (Figure 5c), consistent with previous studies demonstrating that streaming of tumor cells *in vivo* has elevated Mena<sup>INV</sup> expression.<sup>19</sup> In addition, the sensitivity of tumor cells towards HGF was ablated when MTLn3 tumor cells were overexpressing Mena11a (Figure 5c), which was shown previously to reduce streaming migration and metastasis in mammary tumors *in vivo*.<sup>19</sup>

The relative importance of HGF in tumor cell chemotaxis *in vivo* was investigated using the same inhibitors in Figure 4. The ability to collect tumor cells in this assay is a direct measure of directional tumor cell streaming migration *in vivo*.<sup>26,68</sup> Inhibition of tumor cell migration towards the HGF gradient in the *in vivo* invasion assay was achieved by addition of the C-Met inhibitors Altiratinib or PF04217903 or the EGFR inhibitor Iressa and CSF1R inhibitor DCC-3014<sup>14,30,51–54,69–71</sup> (Figure 5d).

Using intravital imaging with dendra photo-conversion as described previously,<sup>16,17,19,47</sup> we were able to measure the number of tumor cells migrating away from the site of photo-conversion inside the primary tumor *in vivo* (Figure 5e). Addition of the C-Met inhibitor completely blocked the 20% of tumor cells that typically migrate in 24 h out of the photo-conversion site in the primary tumor (Figure 5f) and led to an increase in overall cell

counts due to proliferation of stationary tumor cells as documented previously.<sup>47</sup>

We next investigated the requirement of HGF signaling for blood vessel-directed migration of tumor cells *in vivo* using intravital imaging (Figure 5g). We found that robust directed tumor cell migration towards blood vessels was dramatically blocked by C-Met inhibition (Figures 5g and h). In addition, the number of circulating tumor cells was reduced in the presence of C-Met inhibitor (Figure 5i), consistent with the requirement for directed tumor cell migration towards blood vessels for intravasation.<sup>18</sup>

The above *in vitro* and *in vivo* results predict the presence of a gradient of HGF associated with blood vessels *in situ*. To investigate this, immunofluorescent staining for HGF in PyMT tissue sections was performed. Immunofluorescent staining for HGF in PyMT tissue sections demonstrated that a gradient of HGF exists with higher levels of HGF near the vessel (Supplementary Figure S4A). Using the immunofluorescence data, we were able to approximate the average fluorescent intensity of HGF being secreted from the blood vessel as a logarithmic function (Supplementary Figure S4B). Using the logarithmic function, we were able to estimate the concentration of HGF to distances up to 400  $\mu\text{m}$  away from the blood vessel (Supplementary Materials and Methods). At 400  $\mu\text{m}$  away from the blood vessel, the calculated HGF concentration is 23.5 pM, which is close to the KD value of the high-affinity C-MET receptor. These findings match published data demonstrating that gradients in breast tumors can exist up to 300–400  $\mu\text{m}$  away from a point source *in vivo*.<sup>26,72</sup> This calculation demonstrates that tumor cells would be able to sense the HGF secreted by endothelial cells for chemotaxis at this distance.

## DISCUSSION

In mammary tumors, tumor cells exhibit sustained directionality of migration as linear chains of cells, a process called streaming, in association with fibronectin-collagen1 containing fibers towards

**Figure 5.** HGF/C-Met signaling is required for sustained tumor cell directionality *in vivo*. To determine if the *in vitro* findings apply *in vivo*, the *in vivo* invasion assay was performed to measure the efficiency of tumor cell collection, which is a measure of sustained directional migration *in vivo*. **(a)** Results in xenograph MTLn3 mammary tumors in response to the concentration of HGF in the collection needle. Mean  $\pm$  s.e.m.,  $n = 5$  collection points per condition. Fifteen SCID mice with MTLn3 tumors were used altogether for the collections. **(b)** Results in PyMT spontaneous mammary tumors in response to the concentration of HGF in the collection needle. Mean  $\pm$  s.e.m.,  $n = 5$  collection points per condition. Fifteen PyMT mice were used altogether for the collections. **(c)** The overexpression of Mena<sup>INV</sup> in MTLn3 tumors (red line with squares) allows tumor cells to respond to lower concentrations of HGF (HGF concentrations in the collection needle are shown on the X-axis) compared to parental MTLn3 tumors (blue diamond line) and MTLn3 tumor overexpressing Mena11a (green triangle line). Mean  $\pm$  s.e.m.,  $n = 7$  collection points per condition. Fifteen SCID mice with Mena<sup>INV</sup> overexpressing MTLn3 tumors and 15 SCID mice with Mena11a overexpressing MTLn3 tumors were used for collections. **(d)** Inhibition of *in vivo* tumor cell migration in the *in vivo* invasion assay using inhibitors in the collection needle. (1) 1.5 nM HGF; (2) DMSO control with no HGF; (3) 1.5 nM HGF+10 nM CSF1R inhibitor DCC3014; (4) 1.5 nM HGF+1  $\mu\text{M}$  EGFR inhibitor Iressa; (5) 1.5 nM HGF+5  $\mu\text{M}$  C-Met inhibitor Altiratinib; (6) 1.5 nM HGF+7 nM C-Met inhibitor PF04217903. Addition of 10 nM CSF1R inhibitor DCC-3014 or 1  $\mu\text{M}$  EGFR inhibitor Iressa reduces the number of MTLn3 tumor cells collected in the *in vivo* invasion assay, but not to background levels of the DMSO control without HGF. Addition of C-Met inhibitors Altiratinib or PF04217903 reduces the number of MTLn3 tumor cells collected to background levels seen in the DMSO control with no HGF in the needle. Inhibitors were used at concentrations that were previously published to be maximally effective at inhibiting their respective receptors and minimizing off-target effects. Mean  $\pm$  s.e.m., ANOVA  $*P < 0.05$ ,  $**P < 0.01$  relative to bar 1.  $n = 11$  collection points per condition. Fifteen mice in total were used for collection of tumor cells. **(e)** Dendra photo-conversion was used to monitor the effects of C-Met/HGF inhibition in MTLn3 tumors. The number of photoconverted red cells remaining in the photo-converted primary tumor volume after 24 h was imaged in the absence and presence of 10 mg/kg C-Met inhibitor PF-04217903. **(f)** Quantification of the number of photo-converted red cells at (1) 0 h and at (2) 24 h after photo-conversion reveals that C-Met inhibition with 10 mg/kg PF-04217903 reduces the ability of tumor cells that migrate away from the photo-conversion site in the primary tumor. Mean  $\pm$  s.e.m.,  $t$ -test  $*P < 0.05$ .  $N = 6$  fields of view for C-MET inhibited and 15 fields of view for DMSO vehicle control. Three mice per condition were used. **(g)** The migration of MTLn3 tumor cells towards blood vessels was monitored via intravital multiphoton microscopy. H2B-Dendra-MTLn3 tumor cells (green) migrate towards the blood vessel (155 kD Rhodamine Dextran) in control tumors (top panel). The presence of the C-Met inhibitor PF04217903 (bottom panel) inhibited tumor cell migration towards the blood vessel. Yellow arrowhead illustrates tumor cell migration in both conditions. **(h)** Quantification of the number of MTLn3 tumor cells moving towards blood vessels *in vivo* in 50 min intravital time lapse movies reveals inhibition of tumor cell migration towards blood vessels in the presence of the C-Met inhibitor. (1) MTLn3 control; (2) MTLn3 tumor+10 mg/kg C-Met inhibitor PF04217903. Mean  $\pm$  s.e.m.,  $t$ -test  $*P < 0.05$ .  $N = 6$  fields of view per condition. Three mice per condition were used. **(i)** Circulating tumor cells in blood were counted in the presence of the C-Met inhibitor PF04217903 or DMSO vehicle. The number of circulating tumor cells was normalized to the DMSO vehicle control. Quantification reveals a significant reduction of circulating tumor cells when 10 mg/kg of C-Met inhibitor PF04217903 was injected intraperitoneally. (1) MTLn3 control; (2) MTLn3 tumor+10 mg/kg C-Met inhibitor PF04217903. Mean  $\pm$  s.e.m.,  $t$ -test  $*P < 0.05$ .  $N = 11$  mice per condition.

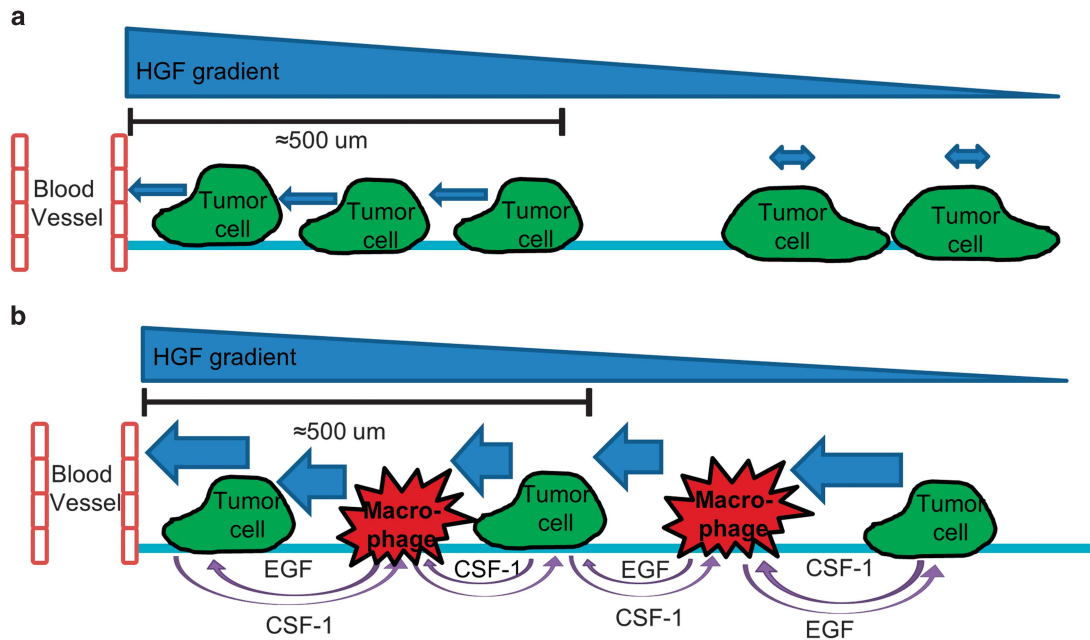


**Figure 6.** Proposed model. (a) Tumor cells that are close to the vessel can migrate towards the endothelial HGF gradient by themselves. (b) However, when tumor cells are more than 500  $\mu\text{m}$  away *in vitro*, the tumor cells require the help of macrophages in order for tumor cells to migrate towards endothelial cells. Macrophages enhance tumor cell sustained directionality in streaming.

blood vessels.<sup>11,15,19,31,47</sup> Previous work also demonstrated that streaming *in vivo* could be partially blocked by inhibiting the CSF-1/EGF paracrine loop to disrupt tumor cell-macrophage interactions.<sup>10,19</sup> However, the question remained—what is the primary signal causing directional migration of tumor cells towards blood vessels in mammary tumors? Our current work answers this question and demonstrates that tumor cells are attracted to endothelial cells in mammary tumors via the HGF/C-Met signaling axis. Using the 1D assay described here, Boyden chambers, and *in vivo* techniques including intra-vital imaging and the *in vivo* invasion assay, HGF/C-Met signaling was implicated as the main signal for sustained directional streaming of tumor cells towards endothelial cells both *in vitro* and *in vivo*. We have also established through immunofluorescent staining and calculations that a gradient of HGF exists to direct tumor cells towards blood vessels *in situ*.

Our *in vitro* results are summarized in the model shown in Figure 6. We have shown that tumor cells within 500  $\mu\text{m}$  of the endothelial cells will chemotactically follow the gradient of endothelial cell released HGF. In the presence of macrophages the distance of response of tumor cells to endothelial HGF is extended to distances greater than 500  $\mu\text{m}$  as the macrophages pair with tumor cells under the control of the EGF/CSF1 paracrine loop, thereby drawing tumor cells into the stream from farther away from the blood vessel. Macrophages also enhance the sustained directional migration of tumor cells towards endothelial cells when tumor cells are 0–500  $\mu\text{m}$  away from the endothelial cells. However, macrophages are not absolutely required for directional migration of tumor cells when close to the endothelium. These findings are in agreement with previous data demonstrating the importance of the EGF/CSF1 paracrine loop in tumor cell streaming.<sup>10,19</sup> Our calculations based on *in situ* data and intravital imaging estimate that tumor cells are able to sense HGF up to 400  $\mu\text{m}$  away from the blood vessel, which matches previously published data that gradients in breast tumors can exist up to 300–400  $\mu\text{m}$  away from the point source.<sup>26,72</sup> This sequence of signaling events *in vitro* and *in vivo* accounts for the observations that macrophages and tumor cells stream together

towards blood vessels *in vivo*, that inhibition of the EGF/CSF1 Paracrine loop can diminish streaming, and that streaming towards blood vessels is most sensitive to inhibition of HGF signaling.

Increased C-Met signaling has been correlated with reduced survival of breast cancer patients.<sup>73–75</sup> This is consistent with our findings that the C-Met signaling pathway mediates the migration of tumor cells towards blood vessels during early steps of dissemination leading to metastasis. Furthermore, we have demonstrated here that tumor cells are sensitized to HGF when the tumor cells are overexpressing Mena<sup>INV</sup> and desensitized when overexpressing Mena11a. These results are in agreement with previous work<sup>9,19,40</sup> demonstrating that Mena<sup>INV</sup> increases the amount of directional streaming and intravasation of tumor cells, leading to increased metastasis, while Mena11a overexpression reduces these tumor cell phenotypes *in vivo*. In addition, our results help to explain why the Mena expression pattern of Mena<sup>INV-high</sup> and Mena11a<sup>low</sup> is correlated with perivascular markers of dissemination including TMEM<sup>20</sup> and predict poor outcome in breast cancer patients.<sup>43,44</sup> Our current work provides additional evidence supporting the recent findings that the Mena<sup>INV-high</sup>/Mena11a<sup>low</sup> expression pattern increases the sensitivity of the EGFR and C-Met receptor.<sup>19,20,41</sup> We postulate that Mena<sup>INV</sup> overexpression is the underlying cause for worse overall disease-free survival in breast cancer patients with the Mena<sup>INV-high</sup>/Mena11a<sup>low</sup> expression pattern because Mena<sup>INV</sup> overexpression increases the sensitivity of the tumor cells to both HGF and EGF, leading to greatly enhanced and sustained directionality of tumor cells towards blood vessels and tumor cell dissemination, both of which have been shown separately to be predictors of poor overall outcome.<sup>73,76</sup>

SDF1 (CXCL12) and its receptor CXCR4 have been documented to be important in tumor cell invasion and motility.<sup>77–82</sup> It is possible that both the SDF1/CXCR4 signaling pathway and HGF/C-Met signaling pathway may work together to attract tumor cells towards the blood vessel. Our current work, however, strongly supports the conclusion that the HGF/C-Met signaling pathway is the main signaling pathway for tumor cell-directed motility

towards blood vessel *in vivo* since inhibition of C-Met dramatically inhibits migration towards blood vessels, as shown here, compared to the relatively partial inhibition of migration towards blood vessels upon inhibition of SDF1/CXCR4 signaling reported previously.<sup>46</sup> Hernandez *et al.* have documented that parental MTLn3 tumor cells do not endogenously express the CXCR4 receptor and only when CXCR4 was artificially overexpressed did parental MTLn3 tumor cells demonstrate a chemotactic response towards SDF1.<sup>46</sup> Our current results support these findings since chemotaxis of tumor cells towards HGF but not SDF1 was observed in cells overexpressing Mena<sup>INV</sup>. In addition, enhanced Mena<sup>INV</sup> expression is found in migrating tumor cells *in vivo*<sup>19,40</sup> and Mena<sup>INV</sup> dramatically increases the sensitivity of these tumor cells towards HGF,<sup>41</sup> supporting our finding that HGF is the main chemotactic factor attracting tumor cells towards blood vessels and ultimately towards the TMEM intravasation sites *in vivo*.

## MATERIALS AND METHODS

### Cell culture

All cell lines used here have been described previously and are detailed in Supplementary Materials and Methods.

### *In vitro* 1D assay

$5 \times 10^3$  MTLn3 tumor cells were plated per well in the CYTOO chamber and labeled with Celltracker dye.  $1 \times 10^3$  macrophages and 10–15 HUVEC beads were plated per well. Inhibitors were added as needed. L15+5% FBS was added until the final volume per well was 200  $\mu$ l. Time-lapse images were obtained on the wide-field DeltaVision microscope (Applied Precision LLC, Issaquah, WA, USA) equipped with a Photometrics CoolSnap HQ2 CCD camera (Photometrics, Tucson, AZ, USA) and NanoMotion III stage (Nanomotion, Ronkonkoma, NY, USA). Tumor cell centroids were tracked for a minimum of 30 frames. Additional details are given in the Supplementary Materials and Methods.

### Transwell assay

$5 \times 10^4$  HUVEC endothelial cells were plated per well in a 24-well plate and  $2.5 \times 10^4$  MTLn3 cells labeled with Celltracker dye were plated in the upper chambers of 8.0  $\mu$ m pore PET Membrane transwells (Falcon 353097, Corning, NY, USA). Cells were allowed to migrate for 16 h towards the bottom well. Cells were fixed with 4% paraformaldehyde and cells in the upper chamber were removed using a cotton swab. Chambers were imaged at  $20\times$  and 8–10 fields per chamber were counted for cells. Ang1, Ang2, VEGF, EGF, CSF1 and SDF1 concentrations were used near the KD values.<sup>83–88</sup>

### Inhibitors and other reagents

Rat recombinant HGF (80429-RNAH) was purchased from Sino-Biological (Beijing, China). Celltracker dye was purchased from Life Technologies (Carlsbad, CA, USA). DCC-3014, Altiratinib and Rebastinib were generously provided by Deciphera (Lawrence, KS, USA). PF04217903 (4239) and Gefitinib (Iressa) was purchased from Tocris (Avonmouth, UK). VEGFR2 blocking antibody (AF357) was purchased from R&D (Minneapolis, MN, USA). Rebastinib was used at the IC<sub>50</sub> value of 5 nM.<sup>57–60,89</sup> VEGFR2 neutralizing antibody was used at the Neutralization-dose-50 (0.25  $\mu$ g/mL).<sup>61–63</sup> PF04217903 was used at Ki 7 nM.<sup>51–53</sup> Altiratinib was used at the IC<sub>50</sub> value of 5 nM.<sup>54</sup> DCC-3014 was used at IC<sub>50</sub> of 10 nM.<sup>69</sup> Iressa was used at 1  $\mu$ M, the optimum concentration for inhibition of EGFR.<sup>14,30,70,71</sup>

### Animal models

*In vivo* studies were performed in PyMT mice and orthotopic tumors derived from injecting MTLn3 cells into SCID mice as previously described.<sup>19</sup> All studies involving mice were carried out in accordance and approved by the Albert Einstein College of Medicine Animal Care and Use Committee.

### *In vivo* invasion assay

Collection of actively migrating cells into needles placed into live anesthetized animals was performed as previously described<sup>135,68,90</sup> except

that rat recombinant HGF was used as a chemoattractant in the needles. Inhibitors to EGFR, CSF1R or C-Met were added with the HGF in the collection needles as listed so that distribution of the drugs was uniformly delivered at the site of measurement.

### Intravital imaging

Intravital multiphoton imaging was performed as described previously<sup>17,19,91</sup> using a custom-built multichannel two-laser microscope previously reported<sup>17</sup> or the Olympus IX70 microscope (Waltham, MA, USA).<sup>31</sup> Details unique to this paper are given in Supplementary Materials and Methods.

### Statistical analysis

Statistical analysis was conducted using one-way ANOVA or unpaired, two-tailed Student's *t*-test. Statistical significance was defined as  $P < 0.05$ . All graphs are displayed as mean  $\pm$  s.e.m. Group size was selected based on cell, reagent or animal limitations while still achieving statistically relevant results. For ANOVA tests, all *P* values were adjusted by not assuming equality of variances.

### CONFLICT OF INTEREST

J Condeelis is a consultant/advisory board member for Deciphera Pharmaceuticals and MetaStat. No potential conflicts of interest were disclosed by the other authors.

### ACKNOWLEDGEMENTS

The authors thank P Guo (Analytical Imaging Facility, Albert Einstein College of Medicine) for technical assistance. They also thank B Smith and D Flynn (Deciphera) for providing Rebastinib, DCC-3014 and Altiratinib. This work was supported by the NCI CA100324, CA150344, the Integrated Imaging Program and the Gruss Lipper Biophotonics Center.

### REFERENCES

- 1 Nguyen DX, Bos PD, Massague J. Metastasis: from dissemination to organ-specific colonization. *Nat Rev Cancer*. 2009; **9**: 274–284.
- 2 Ottewill PD, O'Donnell L, Hoken I. Molecular alterations that drive breast cancer metastasis to bone. *BoneKEY Rep* 2015; **4**: 643.
- 3 Fidler IJ. Critical determinants of metastasis. *Semin Cancer Biol* **12**: 89–96.
- 4 Martins D, Beca F, Schmitt F. 2014. Metastatic breast cancer: mechanisms and opportunities for cytology. *Cytopathology* 2002; **25**: 225–230.
- 5 Talmadge JE, Fidler IJ. AACR centennial series: the biology of cancer metastasis: historical perspective. *Cancer Res* 2010; **70**: 5649–5669.
- 6 Weigelt B, Peterse JL, van 't Veer LJ. Breast cancer metastasis: markers and models. *Nat Rev Cancer* 2005; **5**: 591–602.
- 7 Cancer Genome Atlas N. Comprehensive molecular portraits of human breast tumours. *Nature* 2012; **490**: 61–70.
- 8 Mehlen P, Puisieux A. Metastasis: a question of life or death. *Nat Rev Cancer* 2006; **6**: 449–458.
- 9 Roussos ET, Goswami S, Balsamo M, Wang Y, Stobezki R, Adler E *et al.* Mena invasive (Mena(INV)) and Mena11a isoforms play distinct roles in breast cancer cell cohesion and association with TMEM. *Clin Exp Metastasis* 2011; **28**: 515–527.
- 10 Patsialou A, Wyckoff J, Wang Y, Goswami S, Stanley ER, Condeelis JS. Invasion of human breast cancer cells *in vivo* requires both paracrine and autocrine loops involving the colony-stimulating factor-1 receptor. *Cancer Res* 2009; **69**: 9498–9506.
- 11 Patsialou A, Bravo-Cordero JJ, Wang Y, Entenberg D, Liu H, Clarke M *et al.* Intravital multiphoton imaging reveals multicellular streaming as a crucial component of *in vivo* cell migration in human breast tumors. *Intravital* 2013; **2**: e25294.
- 12 Zhao Z, Zhu X, Cui K, Mancuso J, Federley R, Fischer K *et al.* *In vivo* visualization and characterization of epithelial-mesenchymal transition in breast tumors. *Cancer Res* 2016; **76**: 2094–2104.
- 13 Friedl P, Gilmour D. Collective cell migration in morphogenesis, regeneration and cancer. *Nat Rev Mol Cell Biol* 2009; **10**: 445–457.
- 14 Sharma VP, Beatty BT, Patsialou A, Liu H, Clarke M, Cox D *et al.* Reconstitution of *in vivo* macrophage-tumor cell pairing and streaming motility on one-dimensional micro-patterned substrates. *Intravital* 2012; **1**: 77–85.
- 15 Roussos ET, Condeelis JS, Patsialou A. Chemotaxis in cancer. *Nat Rev Cancer*. 2011; **11**: 573–587.
- 16 Kedrin D, Gligorijevic B, Wyckoff J, Verkhusha VV, Condeelis J, Segall JE *et al.* Intravital imaging of metastatic behavior through a mammary imaging window. *Nat Methods* 2008; **5**: 1019–1021.



- 17 Entenberg D, Wyckoff J, Gligorijevic B, Roussos ET, Verkhusa VV, Pollard JW *et al*. Setup and use of a two-laser multiphoton microscope for multichannel intravital fluorescence imaging. *Nat Protoc* 2011; **6**: 1500–1520.
- 18 Harney AS, Arwert EN, Entenberg D, Wang Y, Guo P, Qian BZ *et al*. Real-time imaging reveals local, transient vascular permeability, and tumor cell intravasation stimulated by TIE2hi macrophage-derived VEGFA. *Cancer Discov* 2015; **5**: 932–943.
- 19 Roussos ET, Balsamo M, Alford SK, Wyckoff JB, Gligorijevic B, Wang Y *et al*. Mena invasive (MenaINV) promotes multicellular streaming motility and trans-endothelial migration in a mouse model of breast cancer. *J Cell Sci* 2011; **124**(Pt 13): 2120–2131.
- 20 Pignatelli J, Goswami S, Jones JG, Rohan TE, Pieri E, Chen X *et al*. Invasive breast carcinoma cells from patients exhibit MenaINV- and macrophage-dependent transendothelial migration. *Sci Signal* 2014; **7**: ra112.
- 21 Magbanua MJ, Das R, Polavarapu P, Park JW. Approaches to isolation and molecular characterization of disseminated tumor cells. *Oncotarget* 2015; **6**: 30715–30729.
- 22 Aguirre-Ghiso JA. Models, mechanisms and clinical evidence for cancer dormancy. *Nat Rev Cancer* 2007; **7**: 834–846.
- 23 Robinson BD, Sica GL, Liu YF, Rohan TE, Gertler FB, Condeelis JS *et al*. Tumor microenvironment of metastasis in human breast carcinoma: a potential prognostic marker linked to hematogenous dissemination. *Clin Cancer Res* 2009; **15**: 2433–2441.
- 24 Oktay MH, Gertler FB, Liu YF, Rohan TE, Condeelis JS, Jones JG. Correlated immunohistochemical and cytological assays for the prediction of hematogenous dissemination of breast cancer. *J Histochem Cytochem*. 2012; **60**: 168–173.
- 25 Rohan TE, Xue X, Lin HM, D'Alfonso TM, Ginter PS, Oktay MH *et al*. Tumor microenvironment of metastasis and risk of distant metastasis of breast cancer. *J Natl Cancer Inst*; e-pub ahead of print 3 June 2014; doi:10.1093/jnci/dju136.
- 26 Wyckoff J, Wang W, Lin EY, Wang Y, Pixley F, Stanley ER *et al*. A paracrine loop between tumor cells and macrophages is required for tumor cell migration in mammary tumors. *Cancer Res* 2004; **64**: 7022–7029.
- 27 Hernandez L, Smirnova T, Kedrin D, Wyckoff J, Zhu L, Stanley ER *et al*. The EGF/CSF-1 paracrine invasion loop can be triggered by heregulin beta1 and CXCL12. *Cancer Res* 2009; **69**: 3221–3227.
- 28 Sidani M, Wyckoff J, Xue C, Segall JE, Condeelis J. Probing the microenvironment of mammary tumors using multiphoton microscopy. *J Mammary Gland Biol Neoplasia* 2006; **11**: 151–163.
- 29 Locker J, Segall JE. Breast cancer: the matrix is the message. *Am J Pathol* 2011; **178**: 966–968.
- 30 Goswami S, Sahai E, Wyckoff JB, Cammer M, Cox D, Pixley FJ *et al*. Macrophages promote the invasion of breast carcinoma cells via a colony-stimulating factor-1/epidermal growth factor paracrine loop. *Cancer Res* 2005; **65**: 5278–5283.
- 31 Patsialou A, Wang Y, Pignatelli J, Chen X, Entenberg D, Oktay M *et al*. Autocrine CSF1R signaling mediates switching between invasion and proliferation downstream of TGFbeta in claudin-low breast tumor cells. *Oncogene* 2015; **34**: 2721–2731.
- 32 Knutsdottir H, Condeelis JS, Palsson E. 3-D individual cell based computational modeling of tumor cell-macrophage paracrine signaling mediated by EGF and CSF-1 gradients. *Integr Biol (Camb)* 2016; **8**: 104–119.
- 33 Sharma VP, Beaty BT, Cox D, Condeelis JS, Eddy RJ. An in vitro one-dimensional assay to study growth factor-regulated tumor cell-macrophage interaction. *Methods Mol Biol* 2014; **1172**: 115–123.
- 34 Wang W, Wyckoff JB, Goswami S, Wang Y, Sidani M, Segall JE *et al*. Coordinated regulation of pathways for enhanced cell motility and chemotaxis is conserved in rat and mouse mammary tumors. *Cancer Res* 2007; **67**: 3505–3511.
- 35 Patsialou A, Wang Y, Lin J, Whitney K, Goswami S, Kenny PA *et al*. Selective gene-expression profiling of migratory tumor cells in vivo predicts clinical outcome in breast cancer patients. *Breast Cancer Res* 2012; **14**: R139.
- 36 Gertler FB, Niebuhr K, Reinhard M, Wehland J, Soriano P. Mena, a relative of VASP and Drosophila enabled, is implicated in the control of microfilament dynamics. *Cell* 1996; **87**: 227–239.
- 37 Loureiro JJ, Rubinson DA, Bear JE, Baltus GA, Kwiatkowski AV, Gertler FB. Critical roles of phosphorylation and actin binding motifs, but not the central proline-rich region, for Ena/vasodilator-stimulated phosphoprotein (VASP) function during cell migration. *Mol Biol Cell* 2002; **13**: 2533–2546.
- 38 Bravo-Cordero JJ, Magalhaes MA, Eddy RJ, Hodgson L, Condeelis J. Functions of cofilin in cell locomotion and invasion. *Nat Rev Mol Cell Biol* 2013; **14**: 405–415.
- 39 Gupton SL, Riquelme D, Hughes-Alford SK, Tadros J, Rudina SS, Hynes RO *et al*. Mena binds alpha5 integrin directly and modulates alpha5beta1 function. *J Cell Biol* 2012; **198**: 657–676.
- 40 Goswami S, Philippart U, Sun D, Patsialou A, Avraham J, Wang W *et al*. Identification of invasion specific splice variants of the cytoskeletal protein Mena present in mammary tumor cells during invasion in vivo. *Clin Exp Metastasis* 2009; **26**: 153–159.
- 41 Hughes SK, Oudin MJ, Tadros J, Neil J, Del Rosario A, Joughin BA *et al*. PTP1B-dependent regulation of receptor tyrosine kinase signaling by the actin-binding protein Mena. *Mol Biol Cell* 2015; **26**: 3867–3878.
- 42 Philippart U, Roussos ET, Oser M, Yamaguchi H, Kim HD, Giampieri S *et al*. A Mena invasion isoform potentiates EGF-induced carcinoma cell invasion and metastasis. *Dev Cell* 2008; **15**: 813–828.
- 43 Forse CL, Agarwal S, Pinnaduwwage D, Gertler F, Condeelis JS, Lin J *et al*. Menacalc, a quantitative method of metastasis assessment, as a prognostic marker for axillary node-negative breast cancer. *BMC Cancer* 2015; **15**: 483.
- 44 Agarwal S, Gertler FB, Balsamo M, Condeelis JS, Camp RL, Xue X *et al*. Quantitative assessment of invasive mena isoforms (Menacalc) as an independent prognostic marker in breast cancer. *Breast Cancer Res* 2012; **14**: R124.
- 45 Ho-Yen CM, Jones JL, Kermorgant S. The clinical and functional significance of c-Met in breast cancer: a review. *Breast Cancer Res* 2015; **17**: 52.
- 46 Hernandez L, Magalhaes MA, Coniglio SJ, Condeelis JS, Segall JE. Opposing roles of CXCR4 and CXCR7 in breast cancer metastasis. *Breast Cancer Res* 2011; **13**: R128.
- 47 Gligorijevic B, Bergman A, Condeelis J. Multiparametric classification links tumor microenvironments with tumor cell phenotype. *PLoS Biol* 2014; **12**: e1001995.
- 48 Wyckoff JB, Wang Y, Lin EY, Li JF, Goswami S, Stanley ER *et al*. Direct visualization of macrophage-assisted tumor cell intravasation in mammary tumors. *Cancer Res* 2007; **67**: 2649–2656.
- 49 Wang W, Goswami S, Lapidus K, Wells AL, Wyckoff JB, Sahai E *et al*. Identification and testing of a gene expression signature of invasive carcinoma cells within primary mammary tumors. *Cancer Res* 2004; **64**: 8585–8594.
- 50 Segall JE, Tyerech S, Boselli L, Masseling S, Helft J, Chan A *et al*. EGF stimulates lamellipod extension in metastatic mammary adenocarcinoma cells by an actin-dependent mechanism. *Clin Exp Metastasis* 1996; **14**: 61–72.
- 51 Eder JP, Vande Woude GF, Boerner SA, LoRusso PM. Novel therapeutic inhibitors of the c-Met signaling pathway in cancer. *Clin Cancer Res* 2009; **15**: 2207–2214.
- 52 Timofeevski SL, McTigue MA, Ryan K, Cui J, Zou HY, Zhu JX *et al*. Enzymatic characterization of c-Met receptor tyrosine kinase oncogenic mutants and kinetic studies with aminopyridine and triazolopyrazine inhibitors. *Biochemistry* 2009; **48**: 5339–5349.
- 53 Underiner TL, Herberich T, Miknyoczki SJ. Discovery of small molecule c-Met inhibitors: evolution and profiles of clinical candidates. *Anticancer Agents Med Chem* 2010; **10**: 7–27.
- 54 Smith BD, Kaufman MD, Leary CB, Turner BA, Wise SC, Ahn YM *et al*. Altiratinib inhibits tumor growth, invasion, angiogenesis, and microenvironment-mediated drug resistance via balanced inhibition of MET, TIE2, and VEGFR2. *Mol Cancer Ther* 2015; **14**: 2023–2034.
- 55 Tajima H, Matsumoto K, Nakamura T. Regulation of cell growth and motility by hepatocyte growth factor and receptor expression in various cell species. *Exp Cell Res* 1992; **202**: 423–431.
- 56 Higuchi O, Mizuno K, Vande Woude GF, Nakamura T. Expression of c-met proto-oncogene in COS cells induces the signal transducing high-affinity receptor for hepatocyte growth factor. *FEBS Lett* 1992; **301**: 282–286.
- 57 Flynn DL, Ahn YM, Berger MSTC, Hood MM, Kaufman MD *et al*. Rebastinib and DCC-2701: Targeting of resistance mechanisms in cancer treatment [abstract]. *ACS National Meeting*; 8 April 2013; New Orleans (abstract MEDI 209).
- 58 Flynn DL, Kaufman MD, Leary CB, Hood MM, Lu WP, Turner BA *et al*. Rebastinib, a selective TIE2 kinase inhibitor, decreases TIE2-expressing macrophages, reduces metastasis, and increases survival in murine cancer models. [abstract]. *AACR Special Conference on Cellular Heterogeneity in the Tumor Microenvironment*; 26 February–1 March 2014; San Diego, CA. AACR: Philadelphia, PA, USA (abstract PR01).
- 59 Smith BD, Hood MM, Kaufman MD, Berger M, Flynn DL, Wise SC. Rebastinib, a small molecule TIE2 kinase inhibitor, prevents primary tumor growth and lung metastasis in the PyMT breast cancer model [abstract]. *Proceedings of the AACR Special Conference on Tumor Invasion and Metastasis*; 20–23 January 2013; San Diego, CA. AACR: Philadelphia, PA, USA (abstract B78).
- 60 Smith BD, Leary CB, Kaufman MD, Hood MM, Lu WP, Turner BA *et al*. Rebastinib in combination with eribulin ablates TIE2-expressing macrophages, reduces metastasis, and increases survival in the PyMT metastatic breast cancer model. *Cancer Res* 2013; **73**(24 Suppl): abstract P4-15-12.
- 61 Eichler W, Yafai Y, Keller T, Wiedemann P, Reichenbach A. PEDF derived from glial Muller cells: a possible regulator of retinal angiogenesis. *Exp Cell Res* 2004; **299**: 68–78.
- 62 Giuliani N, Colla S, Lazzaretti M, Sala R, Roti G, Mancini C *et al*. Proangiogenic properties of human myeloma cells: production of angiopoietin-1 and its potential relationship to myeloma-induced angiogenesis. *Blood* 2003; **102**: 638–645.
- 63 Minami T, Yano K, Miura M, Kobayashi M, Suehiro J, Reid PC *et al*. The Down syndrome critical region gene 1 short variant promoters direct vascular



- bed-specific gene expression during inflammation in mice. *J Clin Invest* 2009; **119**: 2257–2270.
- 64 Araki H, Katayama N, Yamashita Y, Mano H, Fujieda A, Usui E et al. Reprogramming of human postmitotic neutrophils into macrophages by growth factors. *Blood* 2004; **103**: 2973–2980.
- 65 Desmarais V, Yamaguchi H, Oser M, Soon L, Mouneimne G, Sarmiento C et al. N-WASP and cortactin are involved in invadopodium-dependent chemotaxis to EGF in breast tumor cells. *Cell Motil Cytoskeleton* 2009; **66**: 303–316.
- 66 Mouneimne G, DesMarais V, Sidani M, Scemes E, Wang W, Song X et al. Spatial and temporal control of cofilin activity is required for directional sensing during chemotaxis. *Curr Biol* 2006; **16**: 2193–2205.
- 67 Sidani M, Wessels D, Mouneimne G, Ghosh M, Goswami S, Sarmiento C et al. Cofilin determines the migration behavior and turning frequency of metastatic cancer cells. *J Cell Biol* 2007; **179**: 777–791.
- 68 Wyckoff J, Gligorijevic B, Entenberg D, Segall J, Condeelis J. The in vivo invasion assay: preparation and handling of collection needles. *Cold Spring Harb Protoc* 2011; **2011**: 1232–1234.
- 69 Smith BD, Kaufman MD, Leary CB, Hood MM, Lu W-P, Turner BA et al. Abstract A53: the specific FMS kinase inhibitor, DCC-3014, durably inhibits FMS kinase in vivo and blocks cancer bone invasiveness. *Cancer Res* 2015; **75**(1 Supplement): A53–A53.
- 70 Yamaguchi H, Lorenz M, Kempki S, Sarmiento C, Coniglio S, Symons M et al. Molecular mechanisms of invadopodium formation: the role of the N-WASP-Arp2/3 complex pathway and cofilin. *J Cell Biol* 2005; **168**: 441–452.
- 71 Anderson NG, Ahmad T, Chan K, Dobson R, Bundred NJ. ZD1839 (Iressa), a novel epidermal growth factor receptor (EGFR) tyrosine kinase inhibitor, potently inhibits the growth of EGFR-positive cancer cell lines with or without erbB2 overexpression. *Int J Cancer* 2001; **94**: 774–782.
- 72 Williams JK, Entenberg D, Wang Y, Padgen MR, Clark A, Castracane J et al. Validation of a device for the active manipulation of the tumor microenvironment during intravital imaging. *Intravital* 2015, In Press.
- 73 Lengyel E, Prechtel D, Resau JH, Gauger K, Welk A, Lindemann K et al. c-Met overexpression in node-positive breast cancer identifies patients with poor clinical outcome independent of Her2/neu. *Int J Cancer* 2005; **113**: 678–682.
- 74 Kang JY, Dolled-Filhart M, Ocal IT, Singh B, Lin CY, Dickson RB et al. Tissue microarray analysis of hepatocyte growth factor/Met pathway components reveals a role for Met, matriptase, and hepatocyte growth factor activator inhibitor 1 in the progression of node-negative breast cancer. *Cancer Res* 2003; **63**: 1101–1105.
- 75 Ghossein RA, Dillon DA, D'Aquila T, Rimm EB, Fearon ER, Rimm DL. Expression of c-met is a strong independent prognostic factor in breast carcinoma. *Cancer* 1998; **82**: 1513–1520.
- 76 Casbas-Hernandez P, D'Arcy M, Roman-Perez E, Brauer HA, McNaughton K, Miller SM et al. Role of HGF in epithelial-stromal cell interactions during progression from benign breast disease to ductal carcinoma in situ. *Breast Cancer Res* 2013; **15**: R82.
- 77 Boimel PJ, Smirnova T, Zhou ZN, Wyckoff J, Park H, Coniglio SJ et al. Contribution of CXCL12 secretion to invasion of breast cancer cells. *Breast Cancer Res* 2012; **14**: R23.
- 78 Cassatella MC, Zorzino L, Sandri MT. Single circulating tumor cell profiling: a new perspective for targeted therapy? *Future Oncol* 2012; **8**: 1253–1256.
- 79 Muller A, Homey B, Soto H, Ge N, Catron D, Buchanan M et al. Involvement of chemokine receptors in breast cancer metastasis. *Nature* 2001; **410**: 50–56.
- 80 Brooks JP, Danforth DN, Albert P, Sciuto LC, Smith SL, Camphausen KA et al. Early ipsilateral breast tumor recurrences after breast conservation affect survival: an analysis of the National Cancer Institute randomized trial. *Int J Radiat Oncol Biol Phys* 2005; **62**: 785–789.
- 81 Cabioglu N, Yazici MS, Arun BK, Smith TL, Hortobagyi GN, Price JE et al. Expression of CXCR4 predicts lymph node metastasis in early breast cancer. *J Clin Oncol* 2004; **22**: 841s–841ss.
- 82 Rhodes LV, Short SP, Neel NF, Salvo VA, Zhu Y, Elliott S et al. Cytokine receptor CXCR4 mediates estrogen-independent tumorigenesis, metastasis, and resistance to endocrine therapy in human breast cancer. *Cancer Res* 2011; **71**: 603–613.
- 83 Sawano A, Takahashi T, Yamaguchi S, Aonuma M, Shibuya M. Flt-1 but not KDR/Flk-1 tyrosine kinase is a receptor for placenta growth factor, which is related to vascular endothelial growth factor. *Cell Growth Differ* 1996; **7**: 213–221.
- 84 Hesselgesser J, Liang M, Hoxie J, Greenberg M, Brass LF, Orsini MJ et al. Identification and characterization of the CXCR4 chemokine receptor in human T cell lines: ligand binding, biological activity, and HIV-1 infectivity. *J Immunol* 1998; **160**: 877–883.
- 85 Davis S, Aldrich TH, Jones PF, Acheson A, Compton DL, Jain V et al. Isolation of angiopoietin-1, a ligand for the Tie2 receptor, by secretion-trap expression cloning. *Cell* 1996; **87**: 1161–1169.
- 86 Maisonnier PC, Suri C, Jones PF, Bartunkova S, Wiegand SJ, Radziejewski C et al. Angiopoietin-2, a natural antagonist for Tie2 that disrupts in vivo angiogenesis. *Science* 1997; **277**: 55–60.
- 87 Hellen EH, Axelrod D. Kinetics of epidermal growth factor/receptor binding on cells measured by total internal reflection/fluorescence recovery after photobleaching. *J Fluoresc* 1991; **1**: 113–128.
- 88 Wang ZE, Myles GM, Brandt CS, Lioubin MN, Rohrschneider L. Identification of the ligand-binding regions in the macrophage colony-stimulating factor receptor extracellular domain. *Mol Cell Biol* 1993; **13**: 5348–5359.
- 89 Chan WW, Wise SC, Kaufman MD, Ahn YM, Ensinger CL, Haack T et al. Conformational control inhibition of the BCR-ABL1 tyrosine kinase, including the gatekeeper T3151 mutant, by the switch-control inhibitor DCC-2036. *Cancer Cell* 2011; **19**: 556–568.
- 90 Wyckoff JB, Segall JE, Condeelis JS. The collection of the motile population of cells from a living tumor. *Cancer Res* 2000; **60**: 5401–5404.
- 91 Wyckoff J, Gligorijevic B, Entenberg D, Segall J, Condeelis J. High-resolution multiphoton imaging of tumors in vivo. *Cold Spring Harb Protoc* 2011; **2011**: 1167–1184.



This work is licensed under a Creative Commons Attribution-NonCommercial-NoDerivs 4.0 International License. The images or other third party material in this article are included in the article's Creative Commons license, unless indicated otherwise in the credit line; if the material is not included under the Creative Commons license, users will need to obtain permission from the license holder to reproduce the material. To view a copy of this license, visit <http://creativecommons.org/licenses/by-nc-nd/4.0/>

© The Author(s) 2017

Supplementary Information accompanies this paper on the Oncogene website (<http://www.nature.com/onc>)